

3D QUANTITATIVE PREDICTION OF DINGJIASHAN DEPOSIT BASED ON MORPHOLOGICAL ANALYSIS OF GEOLOGICAL INTERFACES

^{1,2}PAN YONG, ¹PENG ZHENGLIN

¹ Asstt Prof., School of Geosciences and Info physics, Central South University, Changsha 410083, China

² Asstt Prof., College of Tan Kah Kee, Xiamen University, Xiamen 363105, China

E-mail: ¹ pan_yong_pan@126.com

ABSTRACT

Based on the studies of geological features and ore-controlling factors of Dingjiashan lead-zinc deposit in Fujian, this study creates 3D modeling for primary geological interfaces and geological body. A 3D morphological extraction computer program is further developed based on 3D TIN data models of geological interfaces, which allows us to analyze 3D morphological analyses regarding stratigraphic interface of unconformity surface and extract corresponding 3D morphological parameters. Through studying quantitative relations between mineralized indexes of 3D space and 3D morphological parameters, we are able to build linear regression prediction models for 3D unit grades and metal content. Our model predicts 123917 tons of unit lead content and 520334 tons of zinc. According to spatial distributive characteristics of predicted results, two 3D prospecting targets are determined, providing important decision-making information for further prospecting.

Keywords: *TIN, Geological Interfaces, 3D Morphological Analysis, Quantitative Prediction, Dingjiashan Deposit.*

1. INTRODUCTION

As economy develops, the shortage of deposit resources is getting more and more severe. Meanwhile, exploration and exploitation of mines become more difficult and require deeper searching, therefore, how to predict concealed ore body becomes the center of study[1]-[2]. 3D visualized prediction of concealed ore body is a new technology that gradually emerges as the quantitative evaluation of mineral resources, the 3D geological modeling and spatial information technology are developing. 3D visualized prediction technology is able to position, quantify, and precisely calculate and evaluate the 3D space of concealed ore deep down of the ore district at a lower cost[3]-[4]. Since the 1990s, a large amount of data of geological minerals and mine production geology have been accumulated regarding Dingjiashan lead-zinc deposit during deposit explorations and mine production processes over a long time. Those data reflect, to some extent, the distribution of Dingjiashan lead-zinc deposit in 3D space, therefore, meeting the data requirement of applying 3D visualized prediction technology of concealed ore[5]-[6]. This paper applies 3D

visualized prediction technology of concealed ore to conduct studies on the 3D visualized prediction of Dingjiashan lead-zinc deposit, which will be a significant practice and demonstration of discovering and detecting concealed ore body deep down at lower cost.

2. GEOLOGICAL BACKGROUND

Dingjiashan lead-zinc deposit is a large deposit on Meixian lead-zinc ore field in Youxi county, Fujian province. It is located at the western area of volcanic fault depression zone in eastern Fujian and the eastern area of Zhenghe-Dapu great deep fault zone that is adjacent to caledonian uplift zone of northwestern Fujian. Due to geological tectonism, many “skylights” on the ground are seen. Meixian “skylight” strata extend towards the northeast. It consists of middle-upper proterozoic erathem Longbeixi formation (Pt₂₋₃l) metamorphic rock strata and Daling formation (Pt₂₋₃dl) metamorphic rock strata, forming a short-axis anticlinorium structure with the axis extending towards the north: the mines are mainly preserved in this axial area of subsidiary anticline in Meixian anticlinorium^[7].

Dingjiashan lead-zinc deposit is a massive sulfide deposit [7]. The three layers of ore body are located in greenschist stratum of upper Longbeixi formation ($Pt_{2-3}l^3$), and the occurrence is flat. The occurrence of ore body and that of ore-bearing strata are consistent. Spatial distributive features of the deposit are consistent with the overall extending feature of the ore-bearing lithologic section. As ore body is dominated by fault structure, its occurrence is consistent with that of fault structure. Located within the contact zone between granite porphyry and wall rock, lead-zinc ore body is strictly dominated by the contact zone, resulting in the complex morphology, and its occurrence is basically consistent with that of the contact zone[5]-[6].

Unconformity surface is widely distributed in the mining area, constituting the main structure dominating the distribution of ore body. On the one hand, Steep dip unconformity structure is the best structure for later reformation of strata bound type lead-zinc deposit, and ore bodies surrounding steep dip unconformity structure tends to get intensely thicker and richer. On the other hand, the concealed uplift structure of ore-bearing rock series under the volcanic cap rocks are helpful prospecting signs, and along the internal contact zone of the uplift structure thick and rich ore body can be expected. When the unconformity surface is steep ($>30^\circ$) and skews with the underlying greenschist stratum at a relatively wide angle, then within a certain range (50-200m) of both sides of unconformity surface there will be favorable conditions for ore-forming.

3. 3D MODELING OF GEOLOGICAL INTERFACES

Since different geological interfaces have great significance in controlling the distribution of ore bodies in Dingjiashan lead-zinc deposit, therefore, 3D modeling of geological interfaces and spatial analysis technology can be applied in quantitatively illustrating main controlling factors of ore body distribution within a deposit. As the basis for the morphological analysis of geological interfaces, 3D modeling of geological interfaces is able to provide direct illustrations of geological interfaces and perform morphological analyses, providing sensory understanding of geographical inferences. The essence of 3D modeling of geological interfaces is using surface models to describe geological interfaces. Among the models currently used in simulating geological interfaces, triangulated irregular network (TIN) model is a primary model[8]-[9].

3.1. Establishing geological database

Before applying collected geological data to the computer, they shall be further processed and converted, for instances: the registration of maps or drawings, the vectorization of the section, the disposal of borehole data, the digitization of geological data and the establishment of database, among which, disposal of borehole data and establishment of database are two key steps.

Borehole data include four major parts: trepanning data, inclinometer data, geological record and sample analysis. When processing data disposal, the following details need special attention: eliminating human error, adding properties and converting into the data format required by 3D geological modeling software.

After abovementioned preliminary processing, all the data shall be stored in access database so as to create a geological database. Introducing the data contained in the geological database into 3D modeling software will create a database in 3D geological modeling software that can be visualized through the 3D software.

3.2 Defining Geological Spaces

The minimum coordinate of geological space is (39618000, 2902000, -1200) while (39627000, 2909000, 600) the maximum, and any space larger than -400m is regarded as a mineralization space. There are two different precisions to divide geological spaces: (1) fine precision - 3D unit dimension is 5m×5m×5m; (2) standard precision - 3D unit dimension is 10m×10m×10m.

3.3 3D modeling Of Geological Interfaces

Based on the geological database created, we create 3D models of the geological body with Vulcan 7.5 software. Boundaries of various geological bodies can be delimited on different geological cross sections before creating wire-frame models and block models of various geological bodies. Established wire-frame models of ore body and stratum are shown as in Figure 1 and 2.

4. 3D MORPHOLOGICAL ANALYSIS OF GEOLOGICAL INTERFACES

4.1 Methods

When 3D modeling of geological interfaces is established based on TIN modeling of geological interfaces, space analysis technology can be applied into computers to analyze models and extract the parameters of all types of 3D morphological forms, providing the foundation for further establishing 3D quantitative prediction models of ore body. 3D

morphological analytical methods of geological interfaces put forward and realized in this paper include: (1) analyzing distance fields of geological interfaces; (2) extracting geometrical morphological parameters of geological interfaces; (3) analyzing morphological trends and fluctuations of geological interfaces.

The main idea of the 3D morphological analysis of geological interfaces based on TIN can be summarized as follows: first, establishing 3D models of geological interfaces; establishing raster model of geological spaces to store visualized expressions of field values and fields; calculating distance fields between spatial points and geological interfaces; further exacting general morphological parameters of geological interfaces according to distance fields, in order to obtain geological factor-fields, such as gradients and angles; finally, analyzing morphological trends and fluctuations and extracting multi-stage trend fluctuations, so as to obtain multi-stage trends and fluctuation factor-fields.

Here, 3D modeling of geological interfaces has been already established based on TIN models created by Vulcan 7.5 software, while 3D modeling of geological space is realized through a self-written program, to extract 3D morphological information of geological interfaces.

4.2 3D Morphological Extraction

As the spatial morphology of unconformity surface in Dingjiashan lead-zinc deposit is somehow related to ore-forming,[7] therefore, applying 3D morphological analysis to quantitatively describe it is of great significance. Our method builds on 3D TIN data models and raster model of geological interfaces created by Vulcan software, and further develops a corresponding computer program based on the 3D morphological extraction calculation method[10]. Therefore, not only can 3D morphological analysis of formation interface of unconformity surface be realized, and corresponding 3D morphological parameters can also be extracted. 3D morphological parameters mainly include: parameters of distance fields from spatial points to geological interfaces, and morphological trends and fluctuation parameters of geological interfaces such as gradients and angles.

4.2.1 Results of distance field analysis

Through the distance field analysis of 3D TIN models of unconformity surface in Dingjiashan lead-zinc deposit, we can represent the minimum distance between unit and unconformity surface as distance field value, and then we will have the

distance field factor index of unconformity surface (set as variable X1), as shown in Figure 3.

The transitional region between greenschist belt (Z_1l^3) and leucocrate belt (Z_1l^2) is the most favorable ore-hosting region for "strata bound type" ore body, while those stratigraphic and lithologic ore-controlling factors can also be described via distance field models of stratigraphic interface. Through distance field analysis of 3D TIN model of stratigraphic interfaces of Z_1l^3 and Z_1l^2 in Dingjiashan lead-zinc deposit, we can represent minimum distance from unit to stratigraphic interfaces of Z_1l^3 and Z_1l^2 as the distance field value, and we will have the distance field factor index of stratigraphic interfaces of Z_1l^3 and Z_1l^2 can be obtained (set as variable X2), as shown in Figure 4.

4.2.2 Extracted results of geometrical and morphological parameters

Steep dip unconformity structure is the most favorable structure for late reformation of strata bound type lead-zinc deposit, because ore bodies surrounding steep dip unconformity structure tends to become intensely thicker and richer, bringing great significance to the extraction of gradient parameters of unconformity surface. Extracted gradient factor index of unconformity surface (set as variable X3) is illustrated in Figure 5. The region where the unconformity surface skews with the underlying greenschist stratum at a relatively wide angle is also favorable for mineralization, therefore, we can use included angle factor index of the unconformity surface (set as variable X4) to describe and calculate it, as the results in Figure 6 demonstrate.

4.2.3 Results of Morphological trend-fluctuation analysis

The main purpose of conducting a morphological trend-fluctuation factor analysis of the unconformity surface is to reveal the influence of unconformity surface fluctuations have on the ore-controlling function of surrounding geological spaces. Given the fact that the space between exploration projects is 100m, and the range of sample variation function analysis of Zn is between 100-200m, we decide 100m and 200m, after many repeated tests, as the radii of interpolation search range of primary and secondary filtering respectively. Then, primary and secondary morphological filtering shall be applied to the original TIN model of the unconformity surface, correspondingly, and we will its primary morphological trend factor index (set as variable X5), its primary morphological fluctuation factor index (set as variable X6), its secondary

morphological trend factor index (set as variable X7), and its secondary morphological fluctuation factor index (set as variable X8). Morphological trend factor index results calculated and extracted are shown in Figure 7, while Figure 8 indicates the morphological fluctuation factor index of unconformity surface.

5. 3D QUANTITATIVE PREDICTION

Through studying the quantitative relation between the indexes of mineralization and those of information indexes of 3D space, concealed ore body contained within the area in study can be positioned and quantitatively predicted. The mineralized variables involved include: (1) *Pb* --- average grade of unit lead; (2) *Zn* --- average grade of unit zinc; (3) *PbMet* --- metal amount of unit lead; (4) *ZnMet* --- metal amount of unit zinc.

Prospecting information index allows us to describe the ore-forming favorability of geological ore controlling factor and illustrate the results of how geological ore-controlling influences distribute throughout 3D geological space. This involves 8 Corresponding prospecting information variables: (1) distance to unconformity surface, *X1*; (2) distance between stratigraphic interfaces of Z_1I^3 and Z_1I^2 , *X2*; (3) unconformity surface gradient, *X3*; (4) included angle of unconformity surface, *X4*; (5) primary fluctuation of unconformity surface, *X5*; (6) secondary fluctuation of unconformity surface, *X6*; (7) primary fluctuation of stratigraphic interface, *X7*; and (8) secondary fluctuation of stratigraphic interface, *X8*. So, if we conduct statistical regression analysis into the mineralized index and prospecting information index and establish the prospecting prediction model, we can quantitatively predict concealed ore body.

5.1 Correlation Analysis

Based on information collected from geological exploration (such as drilling), we used statistical analysis software SPSS 15.0 to statistically analyze four indexes of mineralization and eight indexes of prospecting information of a given unit, and have arrived at the statistical results shown by Table 1.

5.2 Prospecting Prediction Model

Specific relations between indexes of mineralization and those of prospecting information can be expressed through multiple regression models, also known as the prospecting prediction model. Building on the correlative relation between indexes of mineralization and those of prospecting information a given unit, we used SPSS 15.0 software for statistical analysis and have arrived at

the following prediction model of 3D unit grade and metal content. As testing results of linear regression models in Table 2 indicates, the prediction model is significant and can help guide prospecting prediction to a certain extent.

$$Pb = 1.3707 - 0.0018 \times X1 + 0.0142 \times X2 - 0.0227 \times X3 - 0.0026 \times X4 - 0.0014 \times X5 - 0.0035 \times X6 - 0.0115 \times X7 - 0.0124 \times X8$$

$$Zn = 3.8688 - 0.0023 \times X1 + 0.0254 \times X2 - 0.0488 \times X3 - 0.0015 \times X4 - 0.0065 \times X5 - 0.0171 \times X6 - 0.0249 \times X7 - 0.0047 \times X8$$

$$PbMet = 18.2689 - 0.0287 \times X1 + 0.1189 \times X2 - 0.3447 \times X3 + 0.01452 \times X4 - 0.0181 \times X5 - 0.0394 \times X6 - 0.1508 \times X7 - 0.1882 \times X8$$

$$ZnMet = 55.6764 - 0.0371 \times X1 + 0.3582 \times X2 - 0.8254 \times X3 - 0.0571 \times X4 - 0.0696 \times X5 - 0.2551 \times X6 - 0.2966 \times X7 - 0.0916 \times X8$$

5.3 Prediction Results

By putting in the indexes of prospecting information of unknown areas, we can perform predictions of them. Raster model of prediction results for the indexes of unit mineralization *Pb*, *Zn*, *PbMet* and *ZnMet* are shown in Figure 9, 10, 11 and 12, respectively. Unit lead evaluation grade predicted by 3D quantitative prediction model is 0.6817%, while the number of unit is 13037 and the amount of predicted unit lead metal is 123917 tons. Unit zinc evaluation grade predicted is 2.8701%, while the number of unit is 13037 and the amount of predicted unit zinc metal is 520334 tons.

5.4 3D Prospecting Target Delimitation

In delimitating prospecting targets, the following three delimitation principles have been taken into consideration: the principle of minimum volume with maximum ore bearing, the principle of mining right ownership, and that of complete target section. Two 3D prospecting targets were delimited deep down and on the surrounding region of Dingjiashan lead-zinc deposit: ① No. 1 target section; ② No. 2 target section, and 3D spatial distributions of both target sections are shown in Figure 13. No. 1 target section is located at the remote area to the east of Dingjiashan mining area, with an elevation range of 60 to -20m. Predicted average grades of lead and zinc grade are about 0.63% and about 2.81%, respectively; while predicted lead metal amounts of lead metal and zinc metal are 8.6 thousand tons and 34.6 thousand tons, respectively. No. 2 target section seats deeply at southwestern Dingjiashan mining area with an elevation range of -30 to -160m. Predicted average grades of lead and zinc grade are about 0.96%, and about 3.35%,

respectively; while predicted lead metal amounts of lead metal and zinc metal are 49.1 thousand tons and 172.6 thousand tons, respectively. 3D spatial distribution of No. II target section is shown in Figure 13.

6. CONCLUSION

In our study, we have developed a 3D morphological analysis program of geological interfaces based on TIN, illustrated with Dingjiashan lead-zinc deposit in Youxi County, Fujian province. We have conducted morphological analysis of geological interfaces, such as stratigraphic interface and unconformity surface, and extracted various geological and morphological factors of lead-zinc ore-forming. In doing so, we are able to reasonably and quantitatively describe geological phenomena, so as to help mineralization predictions. For example, because steep dip unconformity structure constitutes a favorable factor for ore-forming, if the gradient factor of the unconformity surface is extracted by morphological analysis, it will be easier to locate steep dip gradient area, or to establish the nonlinear function relation between steep dip gradient and ore-forming.

we adopt a 3D morphological analysis of geological interface: first, indexes of space morphology of geological interfaces are extracted based on the building and visualization of 3D TIN modeling of geological interfaces; then, field models of geological ore controlling factors are obtained for further quantitative analysis of geological ore controlling factors. This method is significant for 3D visualized quantitative prediction of concealed ore body.

However, further inspections of drilling projects remain needed for delimitating 3D prospecting target, in order to evaluate the effectiveness of the results of 3D quantitative prediction.

REFERENCES:

- [1] S.L.PENG, J.C.FAN, Y.J.SHAO,etal. "New breakthrough in key technologies of location prediction about deep concealed ore bodies of mine",*The Chinese Journal of Nonferrous Metals*, Vol.22, No. 3,2012,pp.844-854.
- [2] X.C.MAO,Y.H.TANG,J.Q.LAI,etal. "Three Dimensional Structure of Metallogenic Geologic Bodies in the Fenghuangshan Ore Field and Ore-controlling Geological Factors",*Acta Geologica Sinica*, Vol.85, No. 9, 2011, pp.1507-1519.
- [3] L.Q.Yang, J.Deng Q.F.Wang Qingfei.etal. "Coupling effects on gold mineralization of deep and shallow structures in the Northwestern Jiaodong Peninsula,Eastern China",*Acta Geologica Sinica*, Vol.80,No.3,2006, pp. 400-411.
- [4] M.Pan Mao, J.Li, Z.G.Wang ,etal. "Application of 3-D geoscience modeling technology for the estimation of solid mineral reserves", *Acta Geologica Sinica*, Vol.83,No.3, 2009,pp.655-660.
- [5] B.Zhou, L.X.Gu. "Geological characteristics and formation Environment of the meixian massive Sulfide deposit",*Mineral Deposits*, Vol.18,No.2, 1999, pp.100-109.
- [6] D.F.SHI,DeFeng,S.G.ZHANG,S.L.HAN ,etal. "Isotope geochemistry of Dingjiashan Pb-Zn deposit in central Fujian Province and its geological significance",*Mineral Deposits*, Vol.32,No.5, 2013,pp.1003-1010.
- [7] J.S.WU,R.S.HUAN. "Potentials of lead , zinc and silver resources and their prospecting direction at Fengyan , Youxi , Fujian ",*Chinese Geology*, Vol.28,No.12, 2001,pp.13-18.
- [8] X.C.MAO, Y.H.ZOU, J.CHEN,etal. "Three-dimensional visual prediction of concealed ore bodies in the deep and marginal parts of crisis mines: a case study of the Fenghuangshan ore field in Tongling, Anhui, China ",*Geological Bulletin OF China*, Vol.29,No.3, 2010,pp.401-413.
- [9] Q.P.Jia, D.Jia, L.Luo ,etal. "Three dimensional evolutionary models of the Qiongxian Structures,Southwestern Sichuan Basin, China: Evidence from Seismic interpretation and Geomorphology",*Acta Geologica Sinica*, Vol.83,No.2, 2009,pp. 372-385.
- [10] X.C.MAO,Y.ZHAO,Y.H.TANG,etal. "Three-dimensional morphological analysis method for geological interfaces based on TIN and its application",*Journal of Central South University(Science and Technology)*, Vol.44,No.4,2013,pp.1493-1500.

AUTHOR PROFILES:

Panyong is Ph.D. candidate of Central South University. He received the master degree from the Hunan University .Currently, he is a associate professor at College of Tan Kah Kee, Xiamen University. His research interests include GIS and Quantitative

Peng Zhenglin is a research student of of Central South University. His research interests include GIS and 3D geology.

Large Figures/Tables

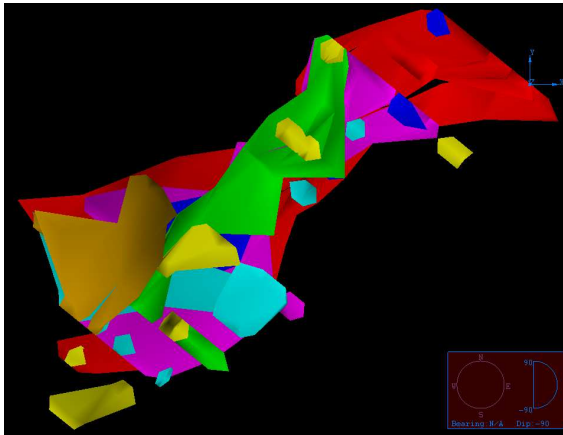


Fig.1 The wire-frame models of ore body

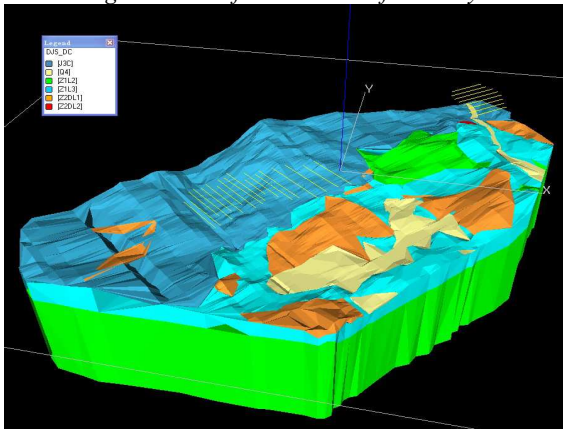


Fig.2 The wire-frame models of stratum

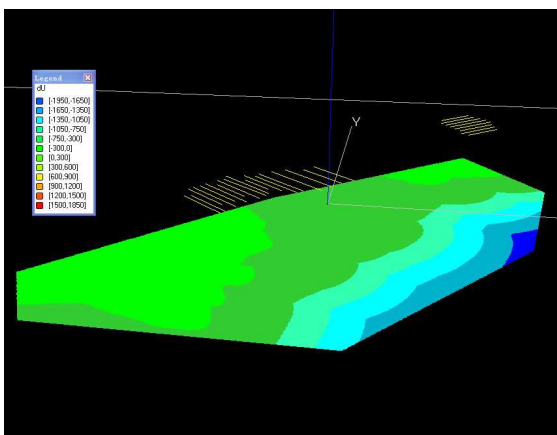


Fig.3 The Distance Field Factor Index Of Unconformity Surface (X1)

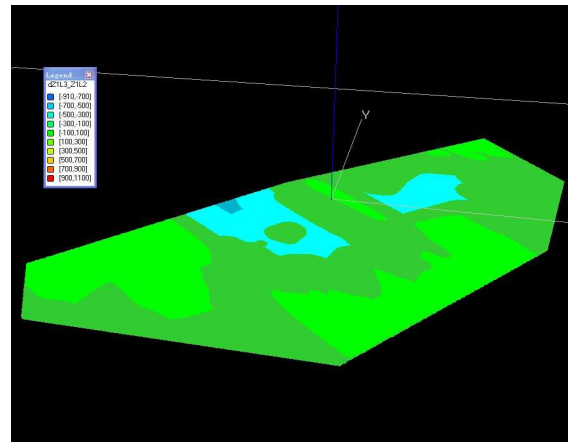


Fig.4 The distance field factor index of stratigraphic interfaces of Z_1l^3 and Z_1l^2 (X2)

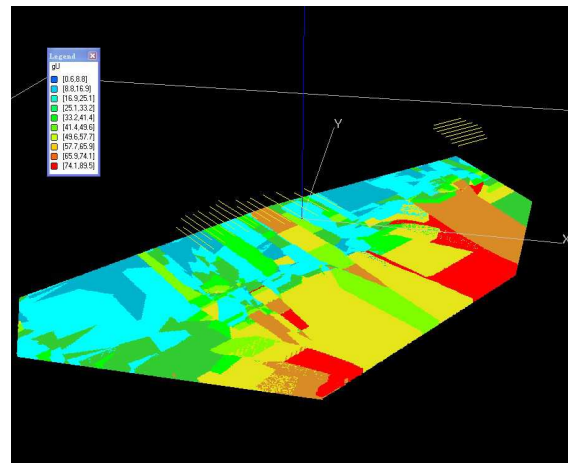


Fig.5 The gradient factor index of unconformity surface (X3)

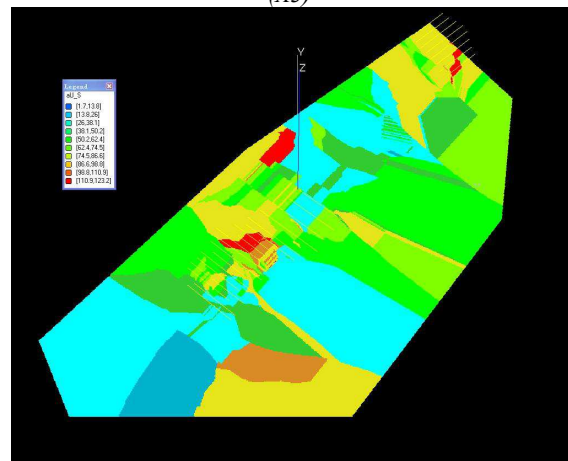


Fig.6 The Angle Factor Index Of The Unconformity Surface (X4)

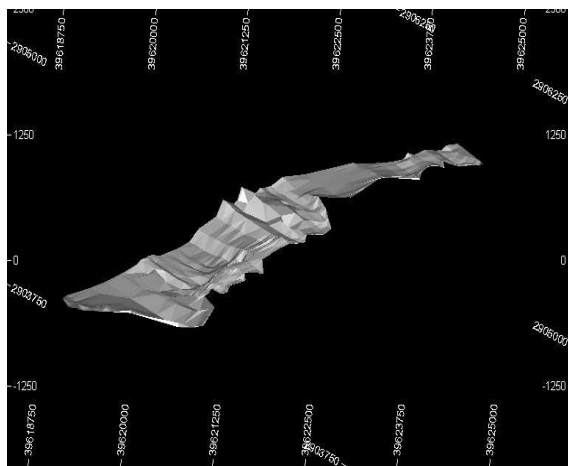


Fig.7a. The Primary Morphological Trend Factor (X5)

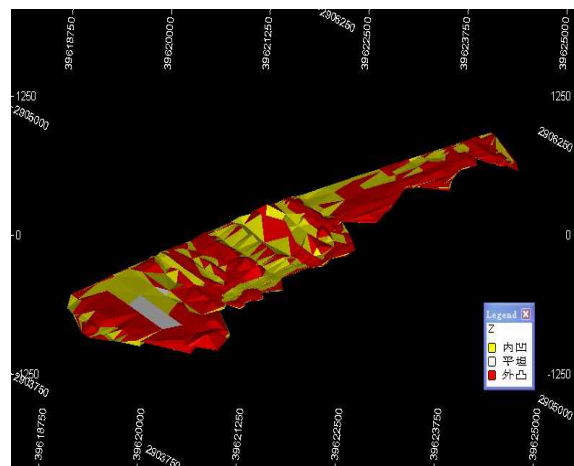


Fig.8b. The Secondary Morphological Fluctuation Factor (X8)

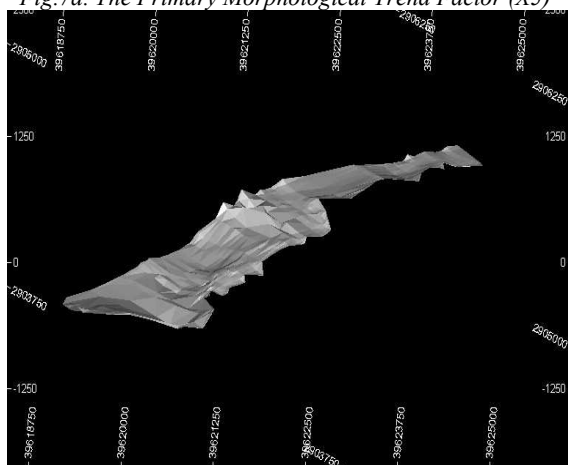


Fig.7b. The Secondary Primary Morphological Trend Factor (X7)

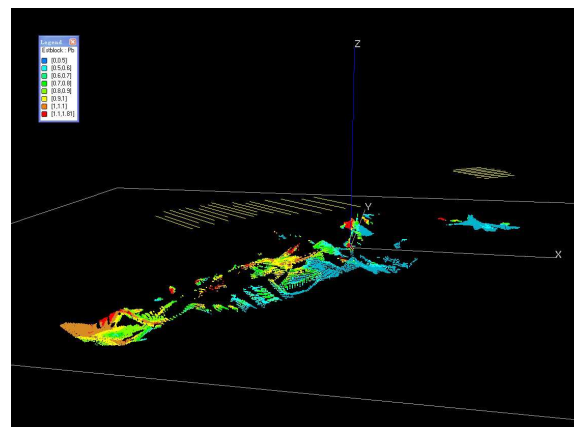


Fig.9 The Prediction Results For The Indexes Of Unit Mineralization Pb

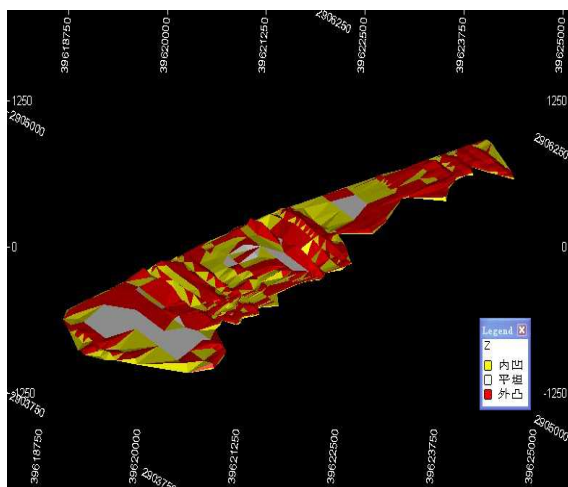


Fig.8a. The Primary Morphological Fluctuation Factor (X6)

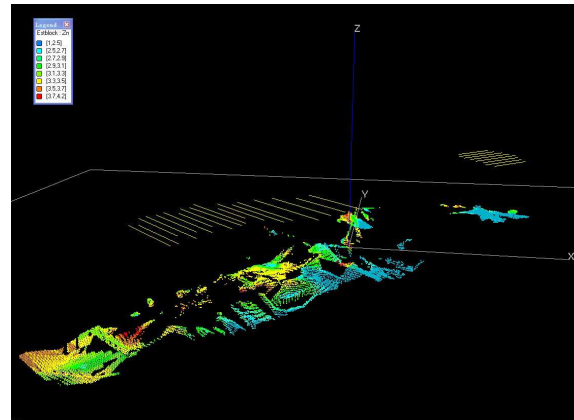


Fig.10 The Prediction Results For The Indexes Of Unit Mineralization Zn

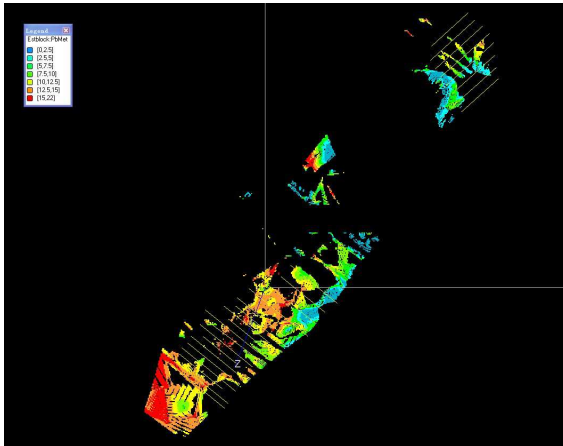


Fig.11 The Prediction Results For The Indexes Of Unit Mineralization Pbmet

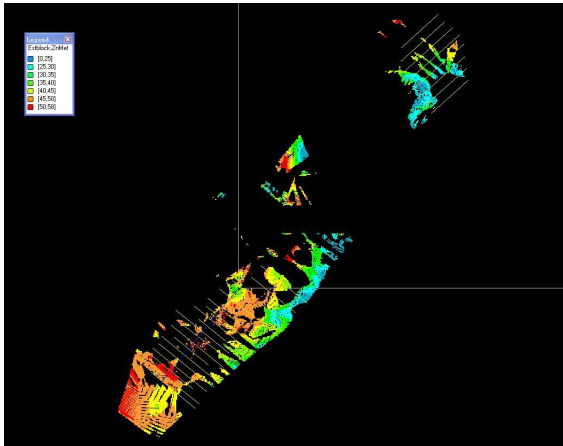


Fig.12 The Prediction Results For The Indexes Of Unit Mineralization Znmet

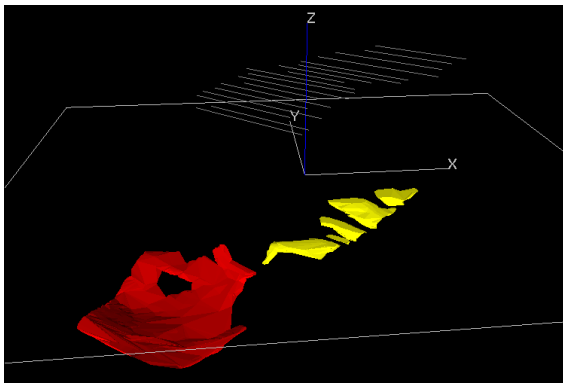


Fig.11 The 3D Spatial Distribution Of Two Targets

Table. 1 The Correlation Coefficients Of Mineralization Indexes And Prospecting Information

	<i>Pb</i>	<i>Zn</i>	<i>PbMet</i>	<i>ZnMet</i>
<i>X1</i>	0.3530	0.4349	0.3192	0.3645
<i>X2</i>	0.1180	0.2056	0.1147	0.1799
<i>X3</i>	0.2640	0.2316	0.2454	0.2131
<i>X4</i>	0.2252	0.2609	0.1863	0.2304
<i>X5</i>	0.2158	0.2879	0.1759	0.2267
<i>X6</i>	0.3452	0.5286	0.3138	0.4381
<i>X7</i>	0.2689	0.2974	0.2290	0.2375
<i>X8</i>	0.2254	0.2613	0.2576	0.2358

Table. 2 The Test Coefficient Of Prediction Model

	R	$F(8,10800)$	$F_{0.05}(8, 10800)$	effectiveness
Pb	0.4665	375.6536	1.94	distinct
Zn	0.5619	622.8343	1.94	distinct
$PbMet$	0.4086	270.5598	1.94	distinct
$ZnMet$	0.4675	377.7287	1.94	distinct